Published in : Colloids and Surfaces B: Biointerfaces (2019), vol. 178, pp. 120–128
DOI: 10.1016/j.colsurfb.2019.02.049
Status : Postprint (Author's version)

ANTI-BIOFOULING ACTIVITY OF RANASPUMIN-2 BIO-SURFACTANT IMMOBILIZED ON CATECHOL-FUNCTIONAL PMMA THIN LAYERS PREPARED BY ATMOSPHERIC PLASMA DEPOSITION

Urszula Czuba[a,b], Robert Quintana[a], Patricia Lassaux[c], Radoslaw Bombera[d], Giacomo Ceccone[d], Jorge Bañuls-Ciscar[d], Maryline Moreno-Couranjou[a], Christophe Detrembleur[b], Patrick Choquet[a]

[a]*Materials Research and Technology Department, Luxembourg Institute of Science and Technology (LIST), L-4422, Belvaux, Luxembourg*

[b]*Center for Education and Research on Macromolecules (CERM), CESAM Research Unit, Chemistry Department, University of Liège, Sart-Tilman B6A, 4000, Liège, Belgium*

[c]*Molecular Biomimetic and Protein Engineering Laboratory (MBPEL), GIGA-R, University of Liège, 4000, Liège, Belgium*

[d]*European Commission, Joint Research Centre (JRC), Ispra, Italy*

Keywords:

Surface functionalization, Plasma polymer, Ranaspumin-2, Surfactant, Catechol, Anti-biofouling surface

Abstract

The deposition of polymeric thin layers bearing reactive functional groups is a promising solution to provide functionality on otherwise inert surfaces, for instance, for bioconjugation purposes. Atmospheric pressure plasma (AP plasma) deposition technology offers many advantages, such as fast deposition rates, low costs, low waste generation and suitability for coating various kind of material surfaces. In this work, the AP plasma-assisted copolymerization of methyl methacrylate (MMA) with a vinyl derivative of L-DOPA was studied in order to deposit coatings with reactive catechol/quinone groups suitable for protein covalent immobilization. The effect of adding a chemical cross-linker, between 0 and 2 mol%, to the monomer mixture is also studied in order to prepare robust plasma PMMA-based layers in liquid physiological media. The layer prepared with 0.2 mol% of cross-linker shows the best balance between stability in saline-buffered media and surface functionalization. Bioconjugation via the grafting of Ranaspumin-2 recombinant, a naturally occurring surfactant protein, is carried out in a single step after plasma deposition. Protein immobilization is corroborated by Quartz Crystal Microbalance with Dissipation (QCM-D) and Surface Plasmon Resonance (SPR) analyses and confirmed via Epicocconone staining, X-Ray Photoemission Spectroscopy (XPS) and Time of Flight Secondary Ion Mass Spectrometry (ToF-SIMS) measurements and surface wettability characterizations. The bio-functionalized layers presented an enhanced activity against the adhesion

Published in : Colloids and Surfaces B: Biointerfaces (2019), vol. 178, pp. 120–128
DOI: 10.1016/j.colsurfb.2019.02.049
Status : Postprint (Author's version)

of Human Serum Albumin (HSA), indicating the grafting potential of the Ranaspumin-2 bio-surfactant to produce anti-biofouling functional coatings.

1. Introduction

Bioconjugation relies on the binding of molecules by covalent or noncovalent bonding mechanisms into a substrate, where at least one of the molecules is of biological origin. This approach is widely used in chemistry, molecular biology and biomedicine to improve the interface properties of well-known materials [1]. The major interest in bioconjugation led to the development of a variety of binding approaches including: protein to protein, polymer to protein, carbohydrate–protein, synthetic labels into biological products (proteins, enzymes antibodies) and protein to inorganic/metallic surfaces [2]. While physical, reversible, adsorption might be the simpler and low-cost approach for bioconjugation, irreversible, covalent binding is preferred for applications requiring long-term performance and extended stability. In particular, the site-specific covalent binding of biomolecules has received great attention for a large variety of biological applications, including drug and gene delivery, biomedicine (diagnostics, implants), imaging and biosensors (bioconjugated quantum dots) [3,4]. Distinctively, this approach leads to minor or no changes in the active form of the biomolecule, which results in stronger ligand binding properties [5]. Polymeric surfaces containing thiol, primary amine, carboxylic acid, maleimide, hydrazide, aldehyde and catechol functional groups [5,6] have been explored for the site-specific covalent binding of proteins through the reaction with lysine, cysteine or tyrosine residues on their N- or C- termini [2,7–9]. Bioconjugation via catechol chemistry has gained more interest since the very successful early works on polydopamine (PDA) deposition to produce non-surface specific adherent coatings rich in catechol units, an approach bio-inspired by the adhesion mechanism of mussel footprint proteins [10–12]. More specifically, L-DOPA and lysine-enriched proteins on mussel footprints were proved to be responsible for their extraordinarily adhesion [13]. Dopamine self-polymerization in a Tris-buffer solution has therefore become a simple method to coat any kind of surface by immersion. These coatings, rich in catechol and quinone moieties, have been proved to promote a site-specific binding of proteins [6,11,14–21] and to have antibacterial properties and low cytotoxicity [17,22–25]. Recently, a dry alternative to PDA wet deposition was presented. Aimed at biomedical applications, atmospheric pressure plasma (AP plasma) deposition technology was employed for the production of functional coatings containing catechol/quinone groups for bioconjugation proposes [26]. The AP plasma-induced free radical polymerization of a dimethacrylate monomer in the presence of catechol-containing methacrylamide comonomer allowed the controlled deposition of thin coatings, with thicknesses ranging from a few to hundreds of nanometres, within minutes, instead of hours, as is usually the case for PDA deposition [22,27]. In addition to the fast deposition rate, the AP plasma polymerization process can work under soft, non-thermal, plasma conditions, which limits monomer fragmentation and increases the retention of functional groups [28,29]. However, an overall softer plasma environment has a more negative impact on the molecular weights than can be achieved, for instance by free radical polymerization. Therefore, polyfunctional monomers are frequently used to increase the resistance of the deposited coatings [30]. In addition, the presence of double-bonds on plasma processes has been shown to increase the polymerization

Published in : Colloids and Surfaces B: Biointerfaces (2019), vol. 178, pp. 120–128
DOI: 10.1016/j.colsurfb.2019.02.049
Status : Postprint (Author's version)

rate, reducing the effect of plasma on the fragmentation and recombination of radicals [31,32]. The stability of any deposited plasma layer in liquid media is an important property for its application in bioconjugation because the layers have to resist the immersion in buffered solutions where the biomolecule immobilization is carried out.

Surfactant proteins are an attractive class of natural surface-active biomolecules with increasing applications in biotechnology [33], for instance, to stabilize water oil emulsions for water decontamination, to create wound healing scaffolds or to modify the wetting properties of implants [1]. Within them, non-lipid globular surfactant proteins, such as fungi-originated hydrophobins, mammalian latherin and ranaspumins found in amphibian nests are especially interesting for their capability to produce biocompatible and biodegradable foams [34–37]. The interactions at the air-water interface of Ranaspumin-2 (Rsn-2, GenBank AY226147) have attracted some specific interest [38]. Despite the amphiphilic nature of its extended polypeptide chain (hydrophobic N-terminus and hydrophilic C-terminus) in aqueous solution, it adopts a tightly folded globular shape of a single helix over a four-stranded sheet with no obvious hydrophobic patches [39]. However, interestingly, at the air-water interface, Rsn-2 induces a conformational clamshell-like change with the exposure of otherwise buried features of the hydrophobic N-terminus [40]. Recently, the surface adhesion properties of Rsn-2 were explored to increase the biocompatibility of hydrophobic surfaces reporting an enhanced cell adhesion [41].

In this work, the site-specific bioconjugation of a Ranaspumin-2 recombinant was explored, aiming to exploit the surface-active properties of this biosurfactant for the preparation of biocompatible and anti-biofouling surfaces. In particular, polymethylmethacrylate layers functionalized with reactive catechol/quinone moieties have been deposited by the AP plasma-induced free radical polymerization method. First, we evaluated the effect of adding a chemical cross-linker to the monomer mixture on the deposition rate, and the stability of the deposited layers in liquid media as well as on the surface concentration of reactive groups. QCM-D and SPR analyses were then carried out to assess the capability of the functional layers for Ranaspumin-2 covalent binding. We also reported on the anti-biofouling performance against adsorption of Human Serum Albumin of the bioconjugated surfaces.

2. Materials and methods

Methyl methacrylate (99% MMA), ethylene glycol dimethacrylate (98% EGDMA) and silver nitrate (> 99% AgNO3) were purchased from Merck. L-DOPA methacrylamide derivative, methyl 3-(3.4-dihydroxyphenyl)-2-(2-methylprop-2-enamido) propanoate (DOMAm) was kindly provided by Symbiose Biomaterials, Belgium. A Serva Purple test (epicocconone staining) set was purchased from Serva, Germany. Silicon wafer substrates (thickness 725 ± 25 µm, P/B, 1–30 Ohm·cm) were cut out and cleaned in an ultrasonic bath, first with Decon90 2%$_{vol}$ solution for 5 min, then with technical grade acetone (3 times, 5 min each) and ethanol absolute (3 times, 5 min each). When necessary, other types of substrates were cleaned in same manner.

Published in : Colloids and Surfaces B: Biointerfaces (2019), vol. 178, pp. 120–128
DOI: 10.1016/j.colsurfb.2019.02.049
Status : Postprint (Author's version)

Ranaspumin 2 recombinant, His_6-Rns2-GC (13.6 kDa), was cloned in pET 28a and produced in *E. coli* BL21DE3. The soluble protein was thus purified on an affinity column thanks to its His-Tag and was submitted to lyophilization.

The coatings were prepared using the Liquid-Assisted Plasma-Enhanced Chemical Vapour Deposition (LA-PECVD) method. The experimental setup for the deposition of plasma polymer layers is shown in **Fig. 1**a and is described elsewhere [26]. Plasma was generated between two horizontal and parallel electrodes, with the grounded electrode being a moving table where the samples to be coated were fixed. The second electrode was formed by two horizontal, high voltage (HV) supply bars covered with thick alumina-dielectric barrier material. Sinusoidal electrical excitation was gained at 10 kHz via a SOFTAL 7010R corona generator at 1.6 W cm^{-2} power with an active plasma zone of 18.72 cm^2. Between the HV supply bars, two discharge gas supply bars were incorporated and aligned perpendicularly to the displacement of the samples. Briefly, the deposition process was started by a surface cleaning and an activation step of sample surfaces by ten-run exposure to a reactive oxygen plasma (5% in argon, 20 slm) at table speed of 10 $mm \cdot min^{-1}$. This step was followed by increasing the table speed to 100 $mm \cdot s^{-1}$ and by switching the plasma gas to argon (20 slm). Each deposition cycle (approx. 8 s) comprised a spraying step and two runs through the plasma zone. The very thin liquid layers of the monomer solutions were sprayed over sample surfaces using a nebulization system (Sono-Tek ultrasonic nozzle-48 kHz, coupled to a Sono-Tek Precision Generator working at 2.9 W) fed by a syringe pump to control the liquid rate. This spray system feed rate needed to be adjusted, depending on the viscosity of the solutions, in order to generate fine mist.

A mechanical profilometer was used to measure the thickness of plasma polymer layers deposited on silicon wafer after scratching. The step-high values of millimeter-long scratches were measured at three different points along the scratch, reporting the average value. The reproducibility of the setup was determined by measuring the thickness of 0.2% EMD layers produced by at least three independent depositions (batches). The FT-IR spectra of the plasma polymer layers deposited on silicon substrates were collected in transmission mode in a Bruker Vertex 70 (4000-800 cm^{-1} range at 4 cm^{-1} resolution using a MCT detector). A Bruker Hyperion 2000 microscope with grazing angle objective coupled to the same spectrophotometer was used to characterize the layers on gold and titanium surfaces. X-Ray Photoelectron Spectroscopy (XPS) analysis was carried out with a Microlab 350 Scanning Auger Microscope with an Al Kα X-ray source (Emission Al Kα1,2 at 1486.6 eV/ PE 20 eV/ TOA 0°). Data analysis and processing was done in CASA XPS (Casa Software Ltd., UK). For each surface, three centrally located points were analysed. A PerkinElmer Lambda 950 UV/ Vis/NIR Spectrophotometer with 100 mm sphere and PMT/InGaAs detector was used to record UV/Vis scans in 200–800 nm range of pivotal points in each sample. The PMT was kept below 861 nm and slit at 2 nm. The fluorescence of samples at an excitation wavelength of 405 nm was recorded by a Zeiss LSM 800 – Airyscan Confocal Microscope equipped with GaAsP detector. Layer stability was assessed by weight change measurements of the deposited layers before and after immersion in PBS buffers at different pH, using a Sartorius ME36-S microbalance (+/- 2 µg). After immersion, the samples were blown-dry with nitrogen and left to dry for 24 h before weighting. The reported weight change values were determined from the average of 3 independent samples. Water contact angle (WCA) measurements were taken in an OCA 15 system (Dataphysics). Static WCA values were determined using the sessile water drop method at room temperature and constant relative humidity. Droplet

Published in : Colloids and Surfaces B: Biointerfaces (2019), vol. 178, pp. 120–128
DOI: 10.1016/j.colsurfb.2019.02.049
Status : Postprint (Author's version)

images were recorded at 1, 2, 3 and 10 s after deposition. Reported WCA values are the average value at 10 s of at least 3 droplets of 2 µl, determined using the Young- Laplace fitting model.

The derivatization of catechol groups by the formation of silver nanoparticles (Ag NP) on the upmost top layer of the plasma polymer layers prepared from DOMAm monomer was described in a previous work [26]. Briefly, the grafting of silver nanoparticles was possible via the oxidation of catechol groups by immersion in $AgNO_3$ solution (1 mg ml^{-1} in milliQ water) for 24 h under gentle agitation. Detection of the grafted Ag NP on the surfaces, after washing in milliQ water (5 times for 5 min each) and drying at room temperature for 24 h, was carried out by environmental scanning electron microscopy (eSEM, Hitachi SEM-SU-70). Three points of each layer were measured via energy-dispersive spectroscopy (EDS) at 1000x magnification. SEM images were then processed in ImageJ software to obtain comparative statistical data relating to the average surface concentration of Ag NPs (NPs μm^{-2}) in each sample. The protein binding on plasma polymer layers was monitored in real-time by a quartz crystal microbalance with energy dissipation monitoring (QCM-D) (QSense Explorer, Biolin Scientific). The flow rate in the measurement system was controlled via peristaltic pump, steady at 100 $\mu L \cdot ml^{-1}$ flow rate. The baseline was determined by 1 h flow of PBS pH8.5 solution with an appropriate ionic strength. Adsorption/grafting of the protein at concentration of 1 mg ml^{-1} in PBS pH8.5 at 22 °C was conducted until the stabilization of the signal (stabilization = δ frequency is lower than 1 Hz /5 min). Afterwards, the system was rinsed with a PBS pH8.5. The sensorgrams obtained from the QCM-D experiments were processed with QSense Dfind. The measurements obtained were expressed in frequency (Δf) and dissipation (ΔD), at the 7th harmonic, in function of time.

Complementary SPR measurements were carried out using Biacore T200 apparatus (GE Healthcare). Gold sensors coated ex-situ with the plasma layers were assembled into the SPR microfluidics, defining 4 individual interaction areas on each sensor, which corresponded to 4 microfluidic channels. Affinity in a single cycle kinetics regime at 0.0001, 0.001, 0.01, 0.1 mg ml^{-1} and grafting kinetics at 1 mg ml^{-1} of biomolecule concentration were performed. All association steps were carried out at a 20 µl min^{-1} flow rate. The baseline was determined by running a PBS pH8.5 (Merck) solution with an appropriate ionic strength. Affinity tests and protein grafting at various concentrations in PBS pH8.5 were conducted at 22 °C. Rinsing steps with PBS pH8.5 were carried at a higher flow rate (100 µl min^{-1}). Non-specific adsorption assays of Human Serum Albumin (HSA) (Merck) were carried out in a similar manner. The measurements resulted in sensorgrams of PR signals, which were expressed in Resonance Units (RU, corrected by the offset value) and drafted according to time. The sensorgrams obtained were processed with dedicated BIAevaluation software (GE Healthcare).

Time of Flight Secondary Ion Mass Spectrometry (ToF-SIMS) analysis was conducted using a reflector type SIMS IV spectrometer (IONTOF GmbH, Münster, Germany) equipped with a 25 keV liquid metal ion gun (LMIG) operating with bismuth primary ions. Spectra were acquired in static mode (primary ion fluence < 10^{12} ions$\cdot cm^{-2}$) in order to preserve the surface molecular information. Charge compensation was applied to the analysis by low-energy (< 20 eV) electron flooding to prevent differential charging of the surface. Mass calibration of ToF-SIMS spectra was obtained by using the peaks C- (12 *m/z*), C_2-(24 *m/z*), C_3- (36 *m/z*), C_4- (48 *m/z*), and C_5- (60 *m/z*) for negative ion and H^+, C^+ (12 *m/z*), CH_3^+ (15 *m/z*), $C_2H_3^+$ (27 *m/z*), $C_3H_5^+$ (41 *m/z*) and $C_4H_7^+$ (55 *m/z*) for positive ion spectra in order to ensure a good relative mass accuracy. Analyses were obtained from a square area of 250 × 250 μm^2 in high mass resolution burst mode (resolution M/ ΔM > 6000). Values of *m/z* are given dimensionless in

Published in : Colloids and Surfaces B: Biointerfaces (2019), vol. 178, pp. 120–128
DOI: 10.1016/j.colsurfb.2019.02.049
Status : Postprint (Author's version)

keeping with IUPAC recommendations, even though m represents the unified atomic mass unit in u. Spectra interpretation was carried out using Surface Lab software v6.4 (ION-TOF GmbH, Münster, Germany). Principal component analysis (PCA) was used to process the ToF-SIMS data in this work. Firstly, ToF-SIMS mass spectra were pre-processed using the Surfacelab software (ION-TOF GmbH). Positive spectra were calibrated using a unique mass calibration list and a peak list was obtained using the peak search tool. Subsequently, a peak list of all mass spectra was exported as a text file for further processing. PCA was performed using the simsMVA app [42]. The text file was loaded into the spectra mode of the simsMVA app where data was normalized by total ion intensity, Poisson-scaled and mean-centred before performing PCA.

Epicocconone staining, Serva Purple (SERVA Electrophoresis GmbH), was conducted for the qualitative verification of the distribution of the protein on the surface, according to the staining protocol provided with the kit. The fluorescence staining results of the samples were obtained as Relative Fluorescence Units.

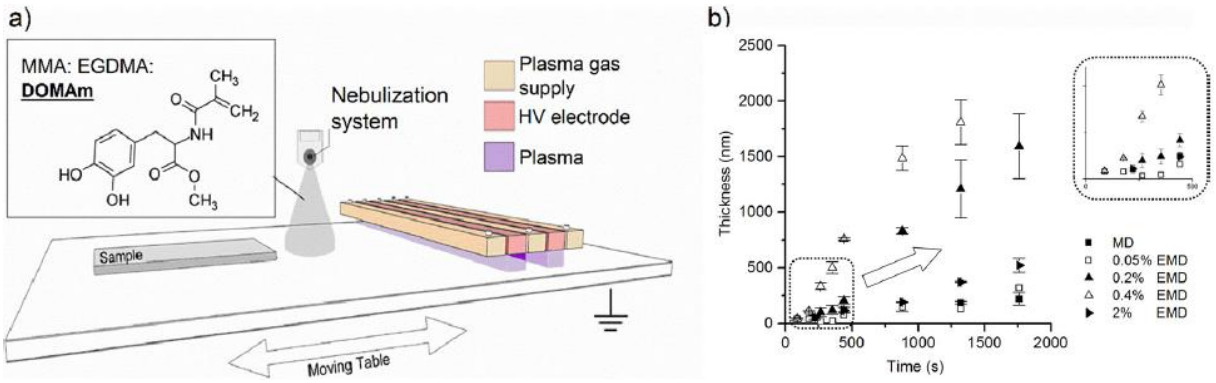

Fig. 1. (a) Scheme of the Liquid-Assisted Plasma Enhanced CVD (LA-PECVD) experimental setup. (b) Thickness vs deposition time on the plasma copolymerization of MMA/DOMAm mixtures with the addition of EGDMA cross-linker, from 0 to 2% molar (error bars: means ± SD (n = 3) for all polymerization times).

3. Results and discussion

3.1. DEPOSITION OF PLASMA POLYMERS LAYERS

The Liquid Assisted – Plasma Enhanced Chemical Vapour Deposition (LA-PECVD) technique was used for the deposition of a series of plasma PMMA thin layers from different mixtures of EGDMA and MMA (EM series), with EGDMA cross-linker content ranging from 0.05 to 2%mol. In addition to this first reference series, a second series of plasma polymer layers was prepared by the plasma copolymerization of the EGDMA cross-linker, MMA, and the functional comonomer, DOMAm (EMD series). It is worth noting that the DOMAm monomer is a powder at room temperature with a relatively low solubility in both MMA and EGDMA (˜2.1 mg ml^{-1}). For all compositions tested, the LA-PECVD technique proved to be an efficient way to deposit polymeric thin films on the metallic and silicon

Published in : Colloids and Surfaces B: Biointerfaces (2019), vol. 178, pp. 120–128
DOI: 10.1016/j.colsurfb.2019.02.049
Status : Postprint (Author's version)

substrates. Pinhole-free thin films fully covering the surface were achieved within minutes and using only a few microlitres of solution.

Table 1 summarizes the feed compositions used for the preparation of the two series of plasma layers, together with their atomic composition, as determined by XPS analyses. The coating thickness evolution curves are shown in **Fig. 1**b. In both series (EM series not reported here), the coating thickness increased steadily as a function of the deposition time. In all cases, the polymerization cycle was kept constant and under 10 s. However, as summarized in **Table 2**, it is necessary to mention that the liquid flow rate was reduced when the cross-linker concentration was increased in the monomer spray solution. This adjustment was needed to produce aerosols with similar physical characteristics, i.e. droplet size, without modifying the input power of the ultrasonic electronic generator. It was found that EGDMA concentration into MMA had a greater effect on the aerosol formation in comparison to the presence of DOMAm. Despite the differences in liquid flow rates within the series, deposition curves already show higher growth rates with increasing EGDMA content in the liquid mixture. For instance, this trend can be clearly observed on the thickness growth curves of 0.2% EMD and 0.4% EMD layers, both of which were produced at a feed rate of 0.1 mL min^{-1}. Otherwise, in order to overcome the effect using different feed rates on the deposition rate, in **Table 2**, the values estimated for the deposition rates and conversion of liquid feed into polymer coating are summarized, having been calculated from the thickness measured after 50 deposition cycles. Interestingly, the addition of EGDMA certainly completely modified the deposition growth mechanism and consequently, significantly increased the deposition rate, for instance, up to 5-fold on the series with 0.4 mol% of cross-linker content. In agreement, this composition also showed the highest conversion of liquid feed into the polymer layer. However, the series with the highest cross-linker content, 2 mol%, did not follow this trend, showing a deposition rate similar to those with low EGDMA content but with a higher liquid to thickness conversion. In comparison with results reported on the free radical polymerization of MMA in the presence of EGDMA by "conventional" wet chemistry [43,44], these plasma polymerization results show similar trends. For instance, Carswell et al. reported that the incorporation of 6 mol% EGDMA increased the reaction rate by up to 3 times with a maximum MMA conversion of 75% [44]. However, they also indicated that lower molar contents of EGDMA, between 1.7 and 3.4 mol%, allowed higher conversions to be obtained, up to 85%. The lower conversion at the higher cross-linker content was then correlated to the Trommsdorff–Norrish effect [45]. This might explain the lower conversion observed in 2% EMD series, which could be also correlated with a change in its deposition growth mechanism.

Spraying techniques as used here, which follow the formation of a very thin liquid layer on the surface, suffer from a selective monomer evaporation and loss of the most volatile monomer (MMA). This phenomenon might have an effect on the actual EGDMA and DOMAm concentration on the surface that participates in the plasma polymerization, in that the concentration is supposed to be higher due to potential losses of MMA because of its vapour pressure, up to 40 fold higher than EGDMA.

Published in : Colloids and Surfaces B: Biointerfaces (2019), vol. 178, pp. 120–128
DOI: 10.1016/j.colsurfb.2019.02.049
Status : Postprint (Author's version)

Table 1

Sample codes and DOMAm concentration in the feed, XPS atomic composition of the deposited layer and catechol surface concentration determined by derivatization with $AgNO_3$.

Sample[d]	[DOMAm] [a]	XPS[b]			Ag° NPs[c] x10
		C1s	O1s	N1s	
PMMA[e]	0	71.4	28.6	0.0	–
MD	2.1	70.0	25.2	4.8	ND
0.05% EM	0	70.2	29.2	0.6	–
0.05% EMD	2.1	66.8	29.2	4.0	9
0.2% EM	0	66.7	32.4	0.9	> 0.1
0.2% EMD	2.1	70.4	27.8	1.8	6
0.4% EM	0	70.0	29.6	0.4	–
0.4% EMD	2.1	70.1	29.2	0.7	1.2
2% EM	0	68.0	31.3	0.7	–
2% EMD	2.1	69.5	29.5	1.0	1.1

[a]DOMAm concentration in the liquid mixture ($mg \cdot ml^{-1}$)

[b]Atomic composition (%atom) of the deposited layer determined from high-resolution XPS spectra.

[c]Surface concentration of silver NPs after derivatization in $NPs \cdot \mu m^{-2}$ determined from SEM images.

[d]Sample code: cross-linker (mol%), E: EGDMA, M: MMA, D: DOMAm.

[e]Value determined from PMMA standard film.

Table 2

Effect of cross-linker content on the deposition of plasma polymer layers by copolymerization with DOMAm.

Sample	Liq. feed rate ($ml\ min^{-1}$)	Deposition rate[a] ($nm\ s^{-1}$)	Liquid to thickness conversion[b]		
			Cycles (num.)	Vol (mL)	Thickness (nm)
MD	0.25	0.3	50	1.8	120
0.05% EMD	0.20	0.2	50	1.5	80
0.2% EMD	0.10	0.5	100	1.5	830
0.4% EMD	0.10	1.7	100	1.5	1490
2% EMD	0.02	0.3	200	0.6	520

[a]Average deposition rate after 50 polymerization cycles.

[b]Volume of liquid pumped to the nebulizer after *n* cycles and its conversion into the deposited polymer plasma layer.

Published in : Colloids and Surfaces B: Biointerfaces (2019), vol. 178, pp. 120–128
DOI: 10.1016/j.colsurfb.2019.02.049
Status : Postprint (Author's version)

3.2. CHARACTERIZATION OF THE PLASMA LAYERS

Deposited polymer plasma layers were investigated by transmission FT-IR, XPS and ToF-SIMS to determine their chemical composition and the retention of functional groups. The presence of ester groups on FTIR spectra was detected by the carbonyl stretch at 1720–1730 cm^{-1} (**Fig. 2**a). A PMMA characteristic C-O absorption band at 1150 cm^{-1} was also detected although it was broader and less well-defined than in the PMMA polymerized by conventional free-radical polymerization. This change in shape is common in PMMA prepared by plasma polymerization [46]. The conversion of vinyl groups by plasma-assisted free radical polymerization was evidenced by the disappearance of the absorption bands at 1638 (C=C), 943 (C–H from $C=CH_3$) and 814 cm^{-1} (=CH_2 skeletal vibration). Considering the detection of the functional monomer units, DOMAm, the absorption bands corresponding to the secondary amide, were identified at 1658 cm^{-1} (carbonyl) and 1520 cm^{-1} (NH scissoring vibration) in the spectra of EMD series. Absorption bands characteristic to DOMAm also appeared at the broad region 3450-3550 cm^{-1} (aromatic C–OH stretching vibrations and NH, not shown), at 1606 cm^{-1} (C–C resonance vibrations in the aromatic ring) and at 1480–1440 cm^{-1} (NH bending/deformation vibration) [47]. Within the EMD series, the intensity of the bands corresponding to DOMAm units decreased by increasing the cross-linker content, despite keeping DOMAm molar concentration in the feed constant through all the series. Taking into consideration the very low vapour pressure of DOMAm, which should prevent its evaporation, the observed trend is likely to be a consequence of a dilution effect promoted by the highest monomer amount converted into a plasma polymer layer when increasing the EGDMA content in the liquid feed, as described in the previous section. This assumption was corroborated by the elemental composition of the upmost top first ˜10 nm of the polymer layers as analysed by XPS (**Table 1**). Within the EMD series (**Fig. 2**b), the nitrogen atomic content, attributed to the amide group in DOMAm (˜399 eV), showed the same trend, as revealed by the transmission FTIR results, which measure the bulk of the plasma polymer layer. As reported previously, the nitrogen content detected on the layers without DOMAm is a consequence of the open, non-concealed, configuration of the plasma reactor and participation of nitrogen from the environment. [26] In addition to XPS, ToF-SIMS analyses were also carried out on 0.2% EM and 0.2% EMD plasma polymer layers. The combination of principal component analysis (PCA) with ToF-SIMS spectra allowed us to distinguish between the two plasma polymer layers. **Fig. 2**c shows the scores plots of the first two principal components (PC1 and PC2) for the two layers, while the corresponding PC1 loadings, showing the mass fragments responsible for the difference, are reported in **Fig. S1**. PC1 was able to detect 84% of sample variance with quite a clear separation of the two different plasma layers. The PC1 of the EMD sample was negatively loaded while the PC1 of EM series was positively loaded. Looking at the loadings, it can be seen that the negative loadings are mostly related to $C_xO_yN_z(H)$ fragments related to the presence of the DOMAm molecule, while the positive loadings can be ascribed to $C_xO_yH_z$ fragments more typical of the methacrylate polymer. The PC2 did not provide more information on the samples as can be seen from the scattering in the scores.

The presence of the chromophore catechol groups of DOMAm in plasma polymer layers was further investigated via their UV–vis absorption and fluorescent properties [26]. **Fig. 2**d shows UV–vis spectra of layers from the EMD series. Catechol detection was attributed to the bands at 220 and 280 nm [48], whose intensity was also found to decrease with the increase of the cross-linker content, in agreement with FTIR and XPS results. Confocal fluorescence microscopy, aimed at the detection and visualization

Published in : Colloids and Surfaces B: Biointerfaces (2019), vol. 178, pp. 120–128
DOI: 10.1016/j.colsurfb.2019.02.049
Status : Postprint (Author's version)

of catechol/quinone moieties in the layers, was also carried out in order to assess their distribution across the surface [49]. As illustrated, in **Fig. 2**d a confocal microscopy image recorded at 475 nm (excitation at 405 nm) of the 0.2% EMD layer is shown. A strong fluorescence intensity from the cathecol/quinone groups is clearly observed. In comparison, the 0.2% EM layer only displayed a slight background fluorescence (**Fig. S2**). Fluorescence intensity correlated well with the catechol/quinone moieties present across the whole surface. The darkest zone in the image, rather than being a consequence of a macroscopic heterogenic distribution of the chromophore units, was ascribed to artefacts due to presence of some buckling in the thin film.

Finally, a quantitative determination of catechol/quinone units in the topmost surface layer was obtained by derivatization using the capacity of catechols to reduce silver ions and form silver nanoparticles (Ag NP) on the surface [26]. In this work, the observation of the Ag NPs by eSEM, after identification using EDS analyses (peaks at 3 and 3.2 keV), was used to estimate their surface concentration (NPs·µm^{-2}). The values reported in **Table 1** show the same trend observed in the EMD series, with a decrease of NPs concentration with the increase of EGDMA content. Nevertheless, the NPs surface concentration on the layer with the highest EGDMA content was significantly higher than the surface concentration of NPs, formed in solution, which can be observed on the layer without DOMAm. For the sake of comparison, the previous reported plasma polymer layer prepared with 100% EGDMA, i.e. without MMA, and the same DOMAm concentration, had a surface concentration of 1.6 NPs µm^{-2} [26].

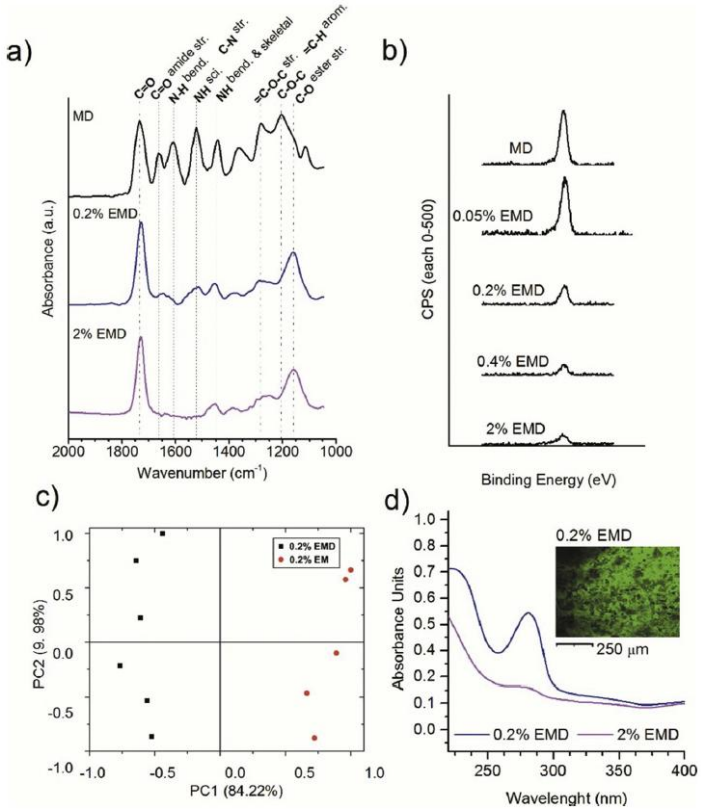

Fig. 2. Transmission FT-IR (a) and (b) N1s high-resolution core level XPS spectra of the EMD plasma polymer layers prepared with different amounts of EGDMA cross-linker. PCA results of ToF-SIMS analysis of plasma layers prepared with 0.2% EGDMA

Published in : Colloids and Surfaces B: Biointerfaces (2019), vol. 178, pp. 120–128
DOI: 10.1016/j.colsurfb.2019.02.049
Status : Postprint (Author's version)

of EM and EMD series: (c) PC1 vs PC2 scores and (d) Detection of chromophore catechol/quinone groups in polymer plasma layers by UV-vis absorption and fluorescence emission.

3.3. STABILITY OF THE PLASMA THIN FILM IN BUFFER MEDIA

Plasma polymers produced from monofunctional monomers with a high degree of functional group retention are usually characterized by low degrees of polymerization [29]. This might affect for instance their stability when immersed in liquid media. In **Fig. 3**, the immersion test results of EMD polymer plasma layers are presented. The results show the remaining weights of the samples after immersion in phosphate-buffered saline (PBS) solution at pH 6 and 8.5 for 15 and 60 min. The two pH selected are well within the range commonly used for biomolecule immobilization assays of catechol-rich surfaces [12,50–52]. The stability of the layers produced without the EGDMA cross-linker and with the lowest assayed amount of 0.05 mol% was significantly affected by the immersion in PBS. Increasing the crosslinking density in the plasma layers led to a huge improvement of their stability. In all cases, the stability in basic media was found to be higher than in a slightly acid environment. This increase in stability might be related to crosslinking polymerization reactions through the self-condensation of quinones or by quinone reaction with catechol, both assisted by catechol oxidation into quinone in basic media [18,53]. These side reactions might also reduce the amount of functional groups available for bioconjugation.

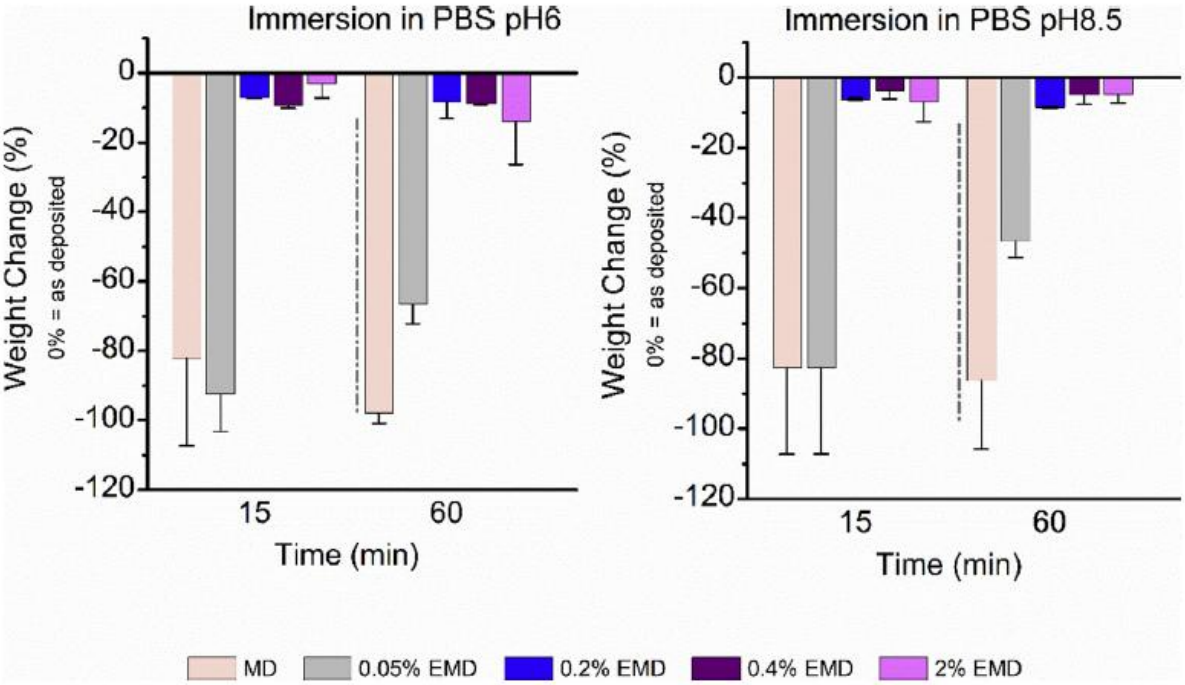

Fig. 3. Stability of the plasma layers on PBS at pH6 and 8.5. Weight change percentage of the dried sample after 15 min and 1 h of immersion (error bars: means ± SD (n = 3)).

3.4. RANASPUMIN-2 (RNS-2) GRAFTING AND ANTI-BIOFOULING PERFORMANCE

The suitability of the plasma EMD polymer layers for bioconjugation assays will largely depend on the amount of reactive catechol/quinone groups available on the surface and their stability in liquid media.

Published in : Colloids and Surfaces B: Biointerfaces (2019), vol. 178, pp. 120–128
DOI: 10.1016/j.colsurfb.2019.02.049
Status : Postprint (Author's version)

In this sense, the 0.2% EMD layer was chosen because of its balance between surface concentration of reactive groups (derivatization results) and stability in the PBS solution. Aiming to provide antibiofouling properties to the plasma layers, bioconjugation was carried out using a biosurfactant protein. In particular, a bioengineered similar of Ranaspumin-2, bearing a cleavable His_6-tag in the N-terminus and a cysteine tag in the C-terminus, abbreviated as His_6-Rns2-GC, was used in this study. In order to favour the formation of the reactive quinone, bioconjugation assays were carried out at pH 8.5 [12]. The presence of the two tags in the Rns-2 similar, with groups reactive towards quinones such as thiol and imidazole, was chosen to increase the covalent immobilization potential of the protein. It was hypothesized that upon absorption at the interface, His_6-Rns2-GC might unhinge its globular structure in solution, adopting an extended conformation with the terminus separated, as has been recently suggested for Rns-2 absorption at both the air-water and liquid-liquid interfaces [38,54]. This unhinged conformation at the polymer/water interface might increase the accessibility of the tags incorporated in Rns-2 for its covalent immobilization onto the surface. The immobilization of His_6-Rns2-GC was first confirmed by QCM-D on sensors coated with a 0.2% EMD plasma polymer layer, as shown in **Fig. 4**a. After the rinsing steps with PBS, a significant amount of injected His_6-Rns2-GC remained on the plasma polymer layer. *Epicocconone* staining (SERVA purple test) was carried out on the sensor surfaces after QCMD assays, which further confirmed the presence of the protein on the biofunctionalized plasma polymer layer (**Fig. 4**b), in addition to showing an even distribution of His_6Rns2-GC all over the surface. An increase of 35°, up to 60°, on the static water contact angle of plasma polymer layers after bioconjugation with His_6-Rns2-GC also indicated the presence of the surfactant protein and the anticipated change on the surface wettability (**Table S1**).

Complementary to QCM-D measurements, Surface Plasmon Resonance (SPR) was used to further examine whether the catechol/ quinone groups incorporated by copolymerization with DOMAm had an influence on interactions with the target protein. In particular, the binding and stability of the protein on the reactive 0.2% EMD plasma layer were investigated and compared against the reference without DOMAm (0.2% EM). **Fig. 5**a shows the SPR sensorgrams of the association and dissociation phases of His_6-Rns2-GC on the polymer plasma layers and on a sensor bare gold surface. Actually, the very strong binding of the protein towards bare gold surface was considered a positive control. Indeed, the SPR response in the equilibrium state was of 3000 RU. The interaction of the protein with the plasma layer without the functional comonomer (0.2% EM) showed fast-binding kinetics during analytes injection (k_{on} = 740 M^{-1} s^{-1}). However, the dissociation phase was characterized by the considerable decrease of the SPR signal, which was dramatically accentuated during the milliQ water washing step. In this case, it is clear that the protein was rather loosely bound to the EM coating and could be easily removed. On the other hand, the interaction with the reactive plasma polymer layer (0,2% EMD) was characterized by slightly slower binding kinetics (k_{on} = 370 M^{-1} s^{-1}) but resulted in a very good stability over the surface. Indeed, the signal only decreased 500 RU, approximately, during the dissociation and washing phases. These results indicate that despite the very similar equilibrium dissociation constant, K_D, 1.9 and 1.6 µM, for EM and EMD layers in PBS, respectively, when the surfaces were washed out with milliQ water, the immobilization of His_6-Rns2-GC seemed more stable on the surface of the catechol/quinone functionalized layer. It might thus be interpreted as the result of a covalent immobilization, which was further evaluated by surface analysis techniques. The presence of the biosurfactant protein was corroborated by XPS (**Table S1**) and ToF-SIMS (**Figure S3**)

Published in : Colloids and Surfaces B: Biointerfaces (2019), vol. 178, pp. 120–128
DOI: 10.1016/j.colsurfb.2019.02.049
Status : Postprint (Author's version)

analyses of the sensors before and after immobilization assays. However, XPS analyses also suggested that the layers without DOMAm were less stable during the SPR assays, as revealed by the detection of Au° from the gold surface on some of the survey spectra (**Figure S4**). Whether or not this result should thus be taken into consideration to accurately interpret SPR binding results between EM and EMD layers, the better stability observed for the bioconjugated catechol/quinone functionalized plasma polymer layer is clearly advantageous for preparing robust biofunctionalized surfaces.

The antibiofouling activity of His_6-Rns2-GC immobilized on 0.2% EMD plasma polymer layers against human serum albumin (HSA) was also assessed by SPR. Fig. 5b shows the sensorgrams of two microfluidic channels on an SPR sensor coated with 0.2% EMD. The biosurfactant protein solution in PBS was injected in one channel (Fc 1) until surface saturation while the other (Fc 3) was run only in PBS. In the absence of the surfactant protein on the surface, HSA binding was effective: after injection, the SPR response increased 1100 RU, followed by a drop in the signal (ΔRU = 450) during PBS rinsing until stabilization. In comparison, the surface grafted with the biosurfactant protein was able to prevent the permanent binding of HSA, as can be observed by a sharp drop in the SPR signal followed by a steady plateau during the dissociation step with PBS.

Interestingly, the anti-biofouling performance of EMD plasma polymer layers functionalized with His_6-Rns2-GC was preserved after ex-situ rinsing and overnight storage in PBS solution.

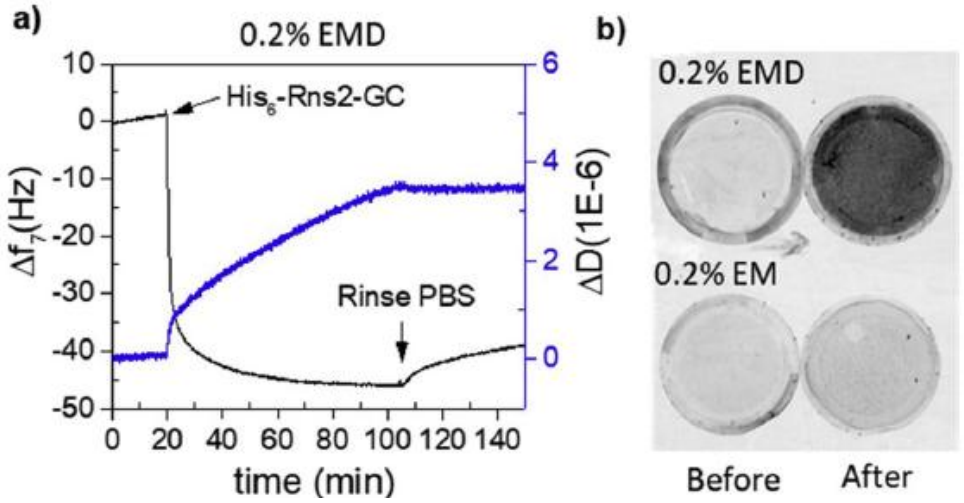

Fig. 4. In situ observation by QCM-D of His_6-Rns2-GC immobilization on 0.2% EMD plasma polymer layer (a). Example of the Epicocconone staining results of sensors coated with 0.2% EMD plasma polymer layer, before and after QCMD assays, to demonstrate the presence of immobilized protein, and comparison with the same layer produced without DOMAm. Before and after images are actually form different quartz sensors but from the same batch (b).

Published in : Colloids and Surfaces B: Biointerfaces (2019), vol. 178, pp. 120–128
DOI: 10.1016/j.colsurfb.2019.02.049
Status : Postprint (Author's version)

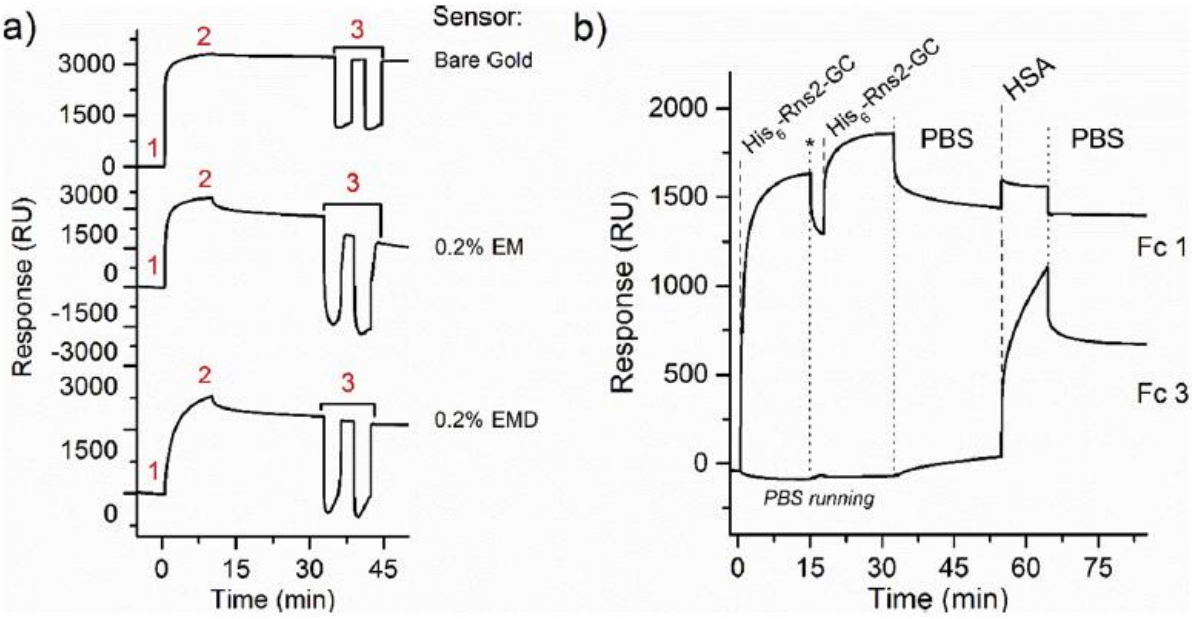

Fig. 5. SPR sensorgrams of (a) His_6-Rns2-GC binding onto sensor surfaces. Protein injection is indicated as 1, protein dissociation in PBS flow as 2 and washing with milliQ water, with an intermediate PBS stabilization step, as 3 and (b) response to the non-specific adsorption of HAS on a 0.2% EMD polymer plasma layer with (Fc 1) and without (Fc 3) surface saturation with His_6-Rns2-GC. Saturation was carried out with a short, intermediate, dissociation step with PBS (*) flow.

4. Conclusions

The atmospheric pressure liquid-assisted plasma polymerization method was successfully carried out for the preparation of reactive functional layers by the copolymerization of methyl methacrylate with the catechol containing the DOMAm monomer. The addition of small amounts of EGDMA, used as chemical cross-linker, has been shown to increase the deposition rate and allow the deposition of stable layers in physiological liquid media, while otherwise their stability would be dramatically compromised. Spectroscopic analyses of the plasma polymer layers revealed the conservation of all anticipated functional groups. However, a decrease in the concentration of DOMAm within the layer and in the upmost top surface was observed when cross-linker content was increased. This unexpected dilution effect was considered to be a consequence of the increase of MMA conversion into the polymer layer promoted by the cross-linker, which at the same time limited MMA evaporation losses during the deposition process. As a consequence, for the application of these layers for bioconjugation, a compromise between surface functionality and stability was anticipated.

A recombinant of Ranaspumin-2, a biocompatible surfactant protein, was immobilized on the reactive functional layer prepared with 0.2 mol% of cross-linker. QCM-D and SPR results revealed a strong and irreversible interaction between the reactive surface and the protein, which might support covalent bioconjugation. Finally, the bioactivated surfaces were challenged with HSA and showed excellent resistance to non-specific adsorption of this plasma protein, proving the antibiofouling activity of the biosurfactant. The results presented here further demonstrate the potential of catechol/quinone

Published in : Colloids and Surfaces B: Biointerfaces (2019), vol. 178, pp. 120–128
DOI: 10.1016/j.colsurfb.2019.02.049
Status : Postprint (Author's version)

containing plasma layers for the development of novel polymeric biomaterial interfaces by site-specific bioconjugation.

Acknowledgements

This research was carried out in the framework of the European MERA.NET METABIO project funded by the Luxembourgish national research fund "Fonds National de la Recherche" (FNR-INTERMAT/13/13) and the DG06-Region Wallonne Agency (no. convention 1318213). The authors would like to thank J. Guillot, J-L Biaggi and S. Cambier from LIST and G. Cotogno from JRC ISPRA for their skilful characterization and valuable discussions. C. Detrembleur is F.R.S.-FNRS Research Director and thanks the FNRS for financial support.

Appendix A. Supplementary data

1. SURFACE ANALYSIS ON SPR SENSOR

Surface Plasmon Resonance (SPR) analyses were conducted in the JRC lab (Italy). There, surface composition of functionalized SPR chips was carried out by XPS and ToF-SIMS equipment sharing the degassing chamber. Samples were mounted on stainless steel bars with a UHV compatible Cu double side tape (3M, USA) and inserted in a load lock chamber for overnight degassing (p=3x10-8 Torr). After degassing the samples were introduced into the XPS and/or ToF-SIMS chamber for analysis. XPS analysis were conducted in a Axis-Ultra-DLD spectrometer (Kratos Analytical, Manchester, UK), using a Kα Al monochromatic source (hv=1486.6 eV) operating at 150 W and X-ray spot size of 400x700 µm2 in hybrid mode. The residual pressure of the analysis chamber during the analysis was less than 8x10−9 Torr. For each sample, both survey spectra (0–1150 eV, pass energy 160 eV) and high-resolution spectra (pass energy at 20 eV) were recorded. Surface charge was compensated by a magnetic charge compensation system and the energy scale was calibrated by setting the C 1s hydrocarbon peak to 285 eV and the Au4f7/2 at 84.00eV. The take-off angle for the acquisitions was 90° with respect to the sample surface. The data were processed using Vision2 software (Kratos Analytical, UK) and the analysis of the XPS peaks was carried out using a commercial software package (Casa XPS v2.3.18PR1, Casa Software Ltd., UK). Peak fitting was performed with no preliminary smoothing. Symmetric Gaussian–Lorentzian (70% Gaussian and 30% Lorentzian) product functions were used to approximate the line shapes of the fitting components after a Shirley-type background subtraction.

Time of Flight Secondary Ion Mass Spectrometry (ToF-SIMS) analysis was conducted using a reflector type SIMS IV spectrometer (ION-TOF GmbH, Münster, Germany) equipped with a 25keV liquid metal ion gun (LMIG) operating with bismuth primary ions. Spectra were acquired in static mode (primary ion fluence < 10^{12} ions·cm^{-2}) in order to preserve the surface molecular information. Charge compensation was applied to the analysis by low-energy (~ 20 25 eV) electron flooding to prevent differential charging of the surface. Mass calibration of ToF-SIMS spectra was obtained by using the peaks C- (12 m/z), C_2- (24 m/z), C_3- (36 m/z), C_4- (48 m/z), and C_5- (60 m/z) for negative ion and H^+, C+

Published in : Colloids and Surfaces B: Biointerfaces (2019), vol. 178, pp. 120–128
DOI: 10.1016/j.colsurfb.2019.02.049
Status : Postprint (Author's version)

(12 m/z), CH_3^+ (15 m/z), $C_2H_3^+$ (27 m/z), $C_3H_5^+$ (41 m/z) and $C_4H_7^+$ (55 m/z) for positive ion spectra in order to ensure a good relative mass accuracy. Analyses were obtained from a square area of 250×250 μm^2 in high mass resolution burst mode (resolution M/ΔM>6000). Values of m/z are given dimensionless in keeping with IUPAC recommendations, even though m represents the unified atomic mass unit in u. Spectra interpretation was carried out using Surface Lab software v6.4 (ION-TOF GmbH, Münster, Germany). Principal component analysis (PCA) was used to process the ToF-SIMS data in this work. Firstly, ToF-SIMS mass spectra were pre-processed using the Surfacelab software (ION-TOF GmbH). Positive spectra were calibrated using a unique mass calibration list and a peak list was obtained using the peak search tool. Subsequently, a peak list of all mass spectra was exported as text file for further processing. PCA was performed using the simsMVA app. The text file was loaded into the spectra mode of simsMVA app where data was normalised by total ion intensity, Poisson scaled and mean centred before 13 performing PCA.

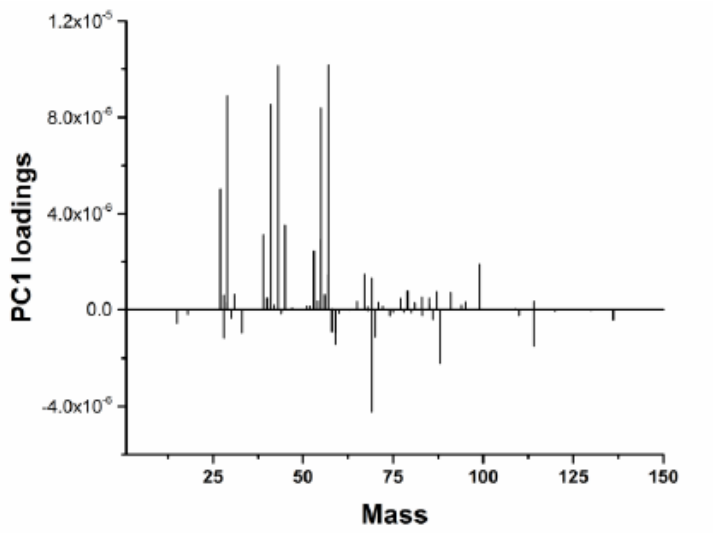

Figure S1. PC1 loadings showing the mass fragments responsible for the difference between 0.2%EM and 0.2%EMD plasma polymer layers in relation with **Figure 2**c in the main manuscript.

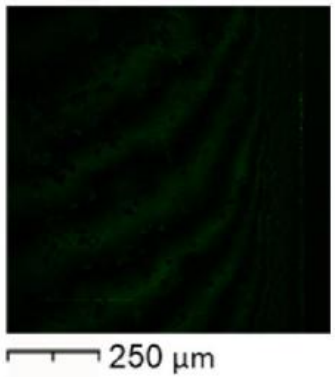

Figure S2. Background fluorescence of the reference 0.2% EM plasma layer, without copolymerization with DOMAm.

Published in : Colloids and Surfaces B: Biointerfaces (2019), vol. 178, pp. 120–128
DOI: 10.1016/j.colsurfb.2019.02.049
Status : Postprint (Author's version)

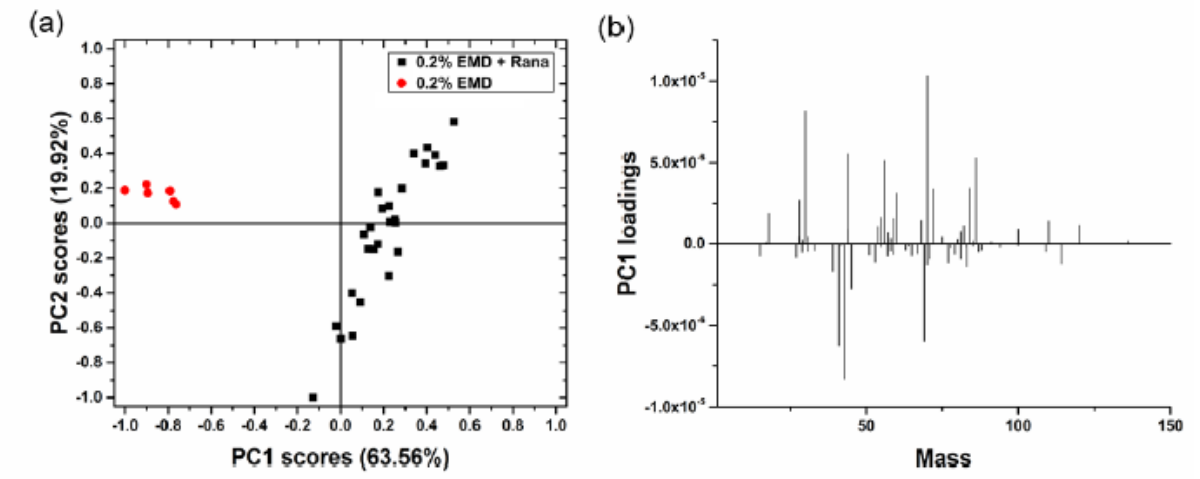

Figure S3. (a) PC1 and PC2 scores of 0.2%EMD and 0.2%EMD+His_6-Rns2-GC samples; (b) corresponding PC1 loadings. PC1 scores separates clearly the two samples. In particular, PC1 is negatively loaded, while the 0.2%EMD +His_6-Rns2-GC score is positively loaded. Looking at the PC1 loadings (b) the positively loaded masses correspond to fragments such as NH_3^+, $C_2H_6N^+$ (m/z=44), $C_3H_6N^+$ (m/z=56), $C_4H_5N_2^+$ (m/z=81) attributable to the 10 biomolecule, whilst the negatively loaded fragments are mostly C_xH_y and $C_xH_yO_z$(N) related to 11 the polymer plasma layer. High mass peaks related to cationized Au(CN, CHN) fragments 12 were also identified.

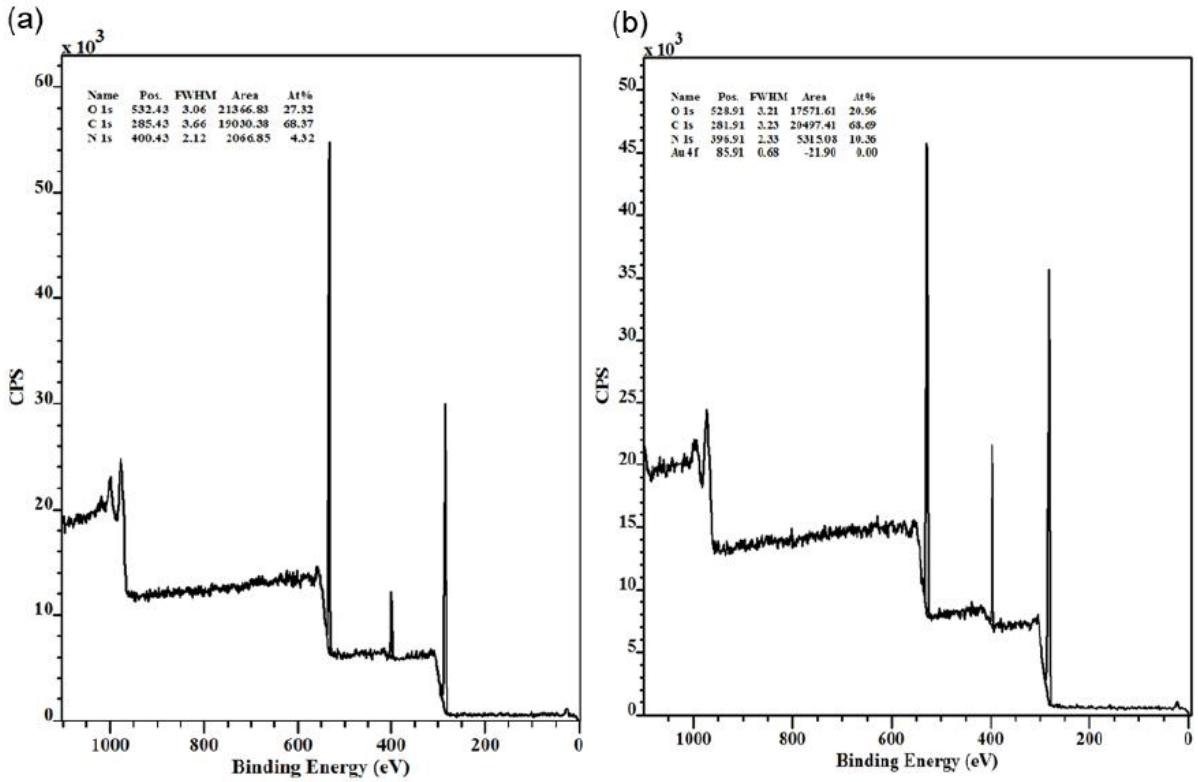

Figure S4. Wide XPS spectra after SPR binding analyses of (a) His_6-Rns2-GC absorbed on SPR gold sensor b) 0.2% EM coated SPR Sensor with His_6-Rns2-GC.

Published in : Colloids and Surfaces B: Biointerfaces (2019), vol. 178, pp. 120–128
DOI: 10.1016/j.colsurfb.2019.02.049
Status : Postprint (Author's version)

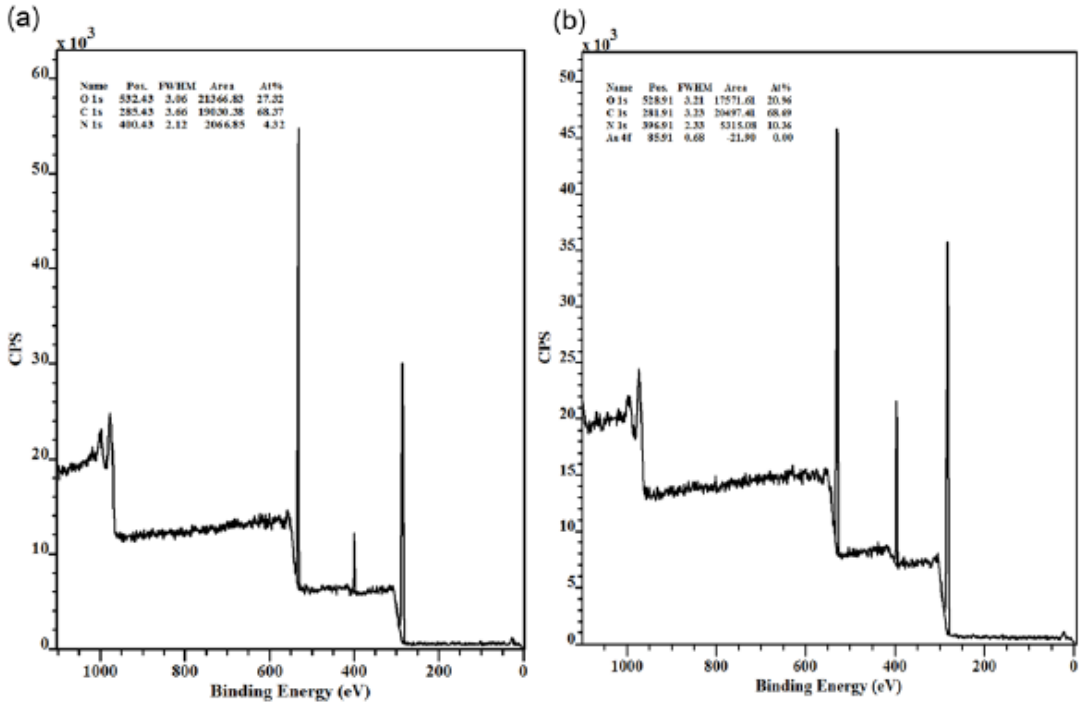

Figure S5. Wide XPS spectra of 0.2% EMD thick layers (>100 nm) deposited on silicon before (a) and after (b) grafting of His_6-Rns2-GC (1 h, protein concentration of 1 mg·ml^{-1} in PBS pH8.5 at 22 °C) and rinsing with PBS pH8.5 and miliQ water.

Table S1. Static water contact angle and XPS composition of the 0.2% EMD layer before and after biosurfactant immobilization.

		XPS (At%)		
Sample	WCA (°)	C1s	O1s	N1s
0.2%EMD	25	67.5	30.8	1.7
0.2%EMD + His_6-Rns2-GC	60	68.4	28.0	3.6
His_6-Rns2-GC[a]	98	72.4	13.5	14.1

[a]Adsorbed in silicon surface.

Published in : Colloids and Surfaces B: Biointerfaces (2019), vol. 178, pp. 120–128
DOI: 10.1016/j.colsurfb.2019.02.049
Status : Postprint (Author's version)

References

[1] M.W. Kennedy, A. Cooper, Surfactant proteins and natural biofoams, in: J.M. Ruso, Á. Piñeiro (Eds.), Proteins Solut. Interfaces Methods Appl. Biotechnol. Mater. Sci. First, John Wiley & Sons, Inc., Hoboken, NJ, USA, 2013, pp. 365–380, , https://doi. org/10.1002/9781118523063.

[2] G.T. Hermanson, Biconjugate Techniques, 2nd ed., (2008).

[3] S. Liebana, G.A. Drago, Bioconjugation and stabilisation of biomolecules in biosensors, Essays Biochem. 60 (2016) 59–68, https://doi.org/10.1042/ EBC20150007.

[4] M. Pereira, E.P. Lai, Capillary electrophoresis for the characterization of quantum dots after non-selective or selective bioconjugation with antibodies for immunoassay, J. Nanobiotechnol. 6 (2008) 10, https://doi.org/10.1186/1477-31556-10.

[5] J. Kalia, R.T. Raines, Advances in Bioconjugation vol. 14, NIH Public Access, 2010, pp. 138–147 https://www.ncbi.nlm.nih.gov/pmc/articles/PMC2901115/pdf/ nihms186498.pdf.

[6] Q.-Y. Hu, F. Berti, R. Adamo, Towards the next generation of biomedicines by site-selective conjugation, Chem. Soc. Rev. 45 (2016) 1691–1719, https://doi.org/10.1039/C4CS00388H.

[7] D. Duday, C. Vreuls, M. Moreno, G. Frache, N.D. Boscher, G. Zocchi, C. Archambeau, C. Van De Weerdt, J. Martial, P. Choquet, Atmospheric pressure plasma modified surfaces for immobilization of antimicrobial nisin peptides, Surf. Coat. Technol. 218 (2013) 152–161, https://doi.org/10.1016/j.surfcoat.2012.12. 045.

[8] A.M. ElSohly, M.B. Francis, Development of oxidative coupling strategies for site-selective protein modification, Acc. Chem. Res. 48 (2015) 1971–1978, https://doi. org/10.1021/acs.accounts.5b00139.

[9] R. Mauchauffé, S. Bonot, M. Moreno-Couranjou, C. Detrembleur, N.D. Boscher, C. Van De Weerdt, A.S. Duwez, P. Choquet, Fast atmospheric plasma deposition of bio-inspired catechol/quinone-rich nanolayers to immobilize NDM-1 enzymes for water treatment, Adv. Mater. Interfaces 3 (2016), https://doi.org/10.1002/admi. 201500520.

[10] J. Sedõ, J. Saiz-Poseu, F. Busqué, D. Ruiz-Molina, Catechol-based biomimetic functional materials, Adv. Mater. 25 (2013) 653–701, https://doi.org/10.1002/ adma.201202343.

[11] H. Lee, S.M. Dellatore, W.M. Miller, P.B. Messersmith, Mussel-inspired surface chemistry for multifunctional coatings, Science (80-.) 318 (2007) 426–430, https:// doi.org/10.1126/science.1147241.

[12] H. Lee, J. Rho, P.B. Messersmith, Facile conjugation of biomolecu les onto surfaces via mussel adhesive protein inspired coatings, Adv. Mater. 21 (2009) 431–434, https://doi.org/10.1002/adma.200801222.

[13] R. Batul, T. Tamanna, A. Khaliq, A. Yu, Recent progress in the biomedical applications of polydopamine nanostructures, Biomater. Sci. 5 (2017) 1204–1229, https://doi.org/10.1039/C7BM00187H.

[14] E. Faure, C. Falentin-Daudré, T.S. Lanero, C. Vreuls, G. Zocchi, C. Van De Weerdt, J. Martial, C. Jérôme, A.-S. Duwez, C. Detrembleur, Functional nanogels as platforms for imparting antibacterial, antibiofilm, and antiadhesion activities to stainless steel, Adv. Funct. Mater. 22 (2012) 5271–5282, https://doi.org/10.1002/adfm. 201201106.

[15] E. Faure, C. Falentin-Daudré, C. Jérôme, J. Lyskawa, D. Fournier, P. Woisel, C. Detrembleur, Catechols as versatile platforms in polymer chemistry, Prog. Polym. Sci. 38 (2013) 236–270, https://doi.org/10.1016/j.progpolymsci.2012.06.004.

[16] Y.H. Ding, M. Floren, W. Tan, Mussel-inspired polydopamine for bio-surface functionalization, Biosurface Biotribology 2 (2016) 121–136, https://doi.org/10.1016/ j.bsbt.2016.11.001.

[17] Z. Jia, P. Xiu, M. Li, X. Xu, Y. Shi, Y. Cheng, S. Wei, Y. Zheng, T. Xi, H. Cai, Z. Liu, Bioinspired anchoring AgNPs onto micro-nanoporous TiO 2 orthopedic coatings: trap-killing of bacteria, surface-regulated osteoblast functions and host responses, Biomaterials 75 (2016) 203–222, https://doi.org/10.1016/j.biomaterials.2015.10. 035.

[18] N. Patil, C. Jérôme, C. Detrembleur, Recent advances in the synthesis of catechol-derived (bio)polymers for applications in energy storage and environment, Prog. Polym. Sci. 82 (2018) 34–91, https://doi.org/10.1016/j.progpolymsci.2018.04. 002.

[19] S. Datta, L.R. Christena, Y.R.S. Rajaram, Enzyme immobilization: an overview on techniques and support materials, 3 Biotech (2012) 1–9, https://doi.org/10.1007/ s13205-012-0071-7.

[20] J. Hasan, R.J. Crawford, E.P. Ivanova, Antibacterial surfaces: the quest for a new generation of biomaterials, Trends Biotechnol. 31 (2013) 295–304, https://doi.org/ 10.1016/j.tibtech.2013.01.017.

Published in : Colloids and Surfaces B: Biointerfaces (2019), vol. 178, pp. 120–128
DOI: 10.1016/j.colsurfb.2019.02.049
Status : Postprint (Author's version)

[21] D. Alves, M. Olívia Pereira, Mini-review: antimicrobial peptides and enzymes as promising candidates to functionalize biomaterial surfaces, Biofouling 30 (2014) 483–499, https://doi.org/10.1080/08927014.2014.889120.

[22] Q. Wei, R. Haag, Universal polymer coatings and their representative biomedical applications, Mater. Horizons 2 (2015) 567–577, https://doi.org/10.1039/ C5MH00089K.

[23] L. Su, Y. Yu, Y. Zhao, F. Liang, X. Zhang, Strong antibacterial polydopamine coatings prepared by a shaking-assisted method, Sci. Rep. 6 (2016) 24420, https://doi.org/10.1038/srep24420.

[24] S.H. Ku, C.B. Park, Human endothelial cell growth on mussel-inspired nanofiber scaffold for vascular tissue engineering, Biomaterials 31 (2010) 9431–9437, https://doi.org/10.1016/j.biomaterials.2010.08.071.

[25] T.S. Sileika, H.-D. Kim, P. Maniak, P.B. Messersmith, Antibacterial Performance of Polydopamine Modified Polymer Surfaces Containing Passive and Active Components, ACS Appl. Mater. Interfaces 3 (2011) 4602–4610, https://doi.org/10.1021/am200978h.

[26] U. Czuba, R. Quintana, M.-C. De Pauw-Gillet, M. Bourguignon, M. Moreno-Couranjou, M. Alexandre, C. Detrembleur, P. Choquet, Atmospheric plasma deposition of methacrylate layers containing catechol/quinone groups: an alternative to polydopamine bioconjugation for biomedical applications, Adv. Healthc. Mater. 7 (2018) 1701059, https://doi.org/10.1002/adhm.201701059.

[27] R. Mauchauffé, M. Moreno-Couranjou, N.D. Boscher, C. Van De Weerdt, A.S. Duwez, P. Choquet, Robust bio-inspired antibacterial surfaces based on the covalent binding of peptides on functional atmospheric plasma thin films, J. Mater. Chem. B Mater. Biol. Med. 2 (2014) 5168, https://doi.org/10.1039/C4TB00503A.

[28] T. Fouquet, G. Mertz, Acrylates and methacrylates: radical polymerization, Encycl. Plasma Technol. (2016) 1–13, https://doi.org/10.1081/E-EPLT-120053955.

[29] F. Loyer, G. Frache, P. Choquet, N.D. Boscher, Atmospheric pressure plasma-initiated chemical vapor deposition (AP-PiCVD) of poly(alkyl acrylates): an experimental study, Macromolecules 50 (2017) 4351–4362, https://doi.org/10.1021/acs. macromol.7b00461.

[30] H. Biederman, Plasma Polymer Films, Published By Imperial College Press and Distributed By World Scientific Publishing Co., 2004, https://doi.org/10.1142/p336.

[31] B. Nisol, A. Batan, F. Dabeux, A. Kakaroglou, I. De Graeve, G. Van Assche, B. Van Mele, H. Terryn, F. Reniers, Surface characterization of atmospheric pressure plasma-deposited allyl methacrylate and acrylic acid based coatings, Plasma Process. Polym. 10 (2013) 564–571, https://doi.org/10.1002/ppap.201200022.

[32] A. Batan, B. Nisol, A. Kakaroglou, I. De Graeve, G. Van Assche, B. Van Mele, H. Terryn, F. Reniers, The impact of double bonds in the APPECVD of acrylate-like precursors, Plasma Process. Polym. (2013), https://doi.org/10.1002/ppap.201300054 n/a-n/a.

[33] A. Cooper, S.J. Vance, B.O. Smith, M.W. Kennedy, Frog foams and natural protein surfactants, Colloids Surf. A Physicochem. Eng. Asp. (2017) 1–10, https://doi.org/ 10.1016/j.colsurfa.2017.01.049.

[34] Cooper, M.W. Kennedy, Biofoams and natural protein surfactants, Biophys. Chem. 151 (2010) 96–104, https://doi.org/10.1016/j.bpc.2010.06.006.

[35] D. Cavalcante Hissa, G. Arruda Bezerra, R. Birner-Gruenberger, L. Paulino Silva, I. Usõn, K. Gruber, V.M. MacIel Melo, Unique crystal structure of a novel surfactant protein from the foam nest of the frog leptodactylus vastus, ChemBioChem 15 (2014) 393–398, https://doi.org/10.1002/cbic.201300726.

[36] M. Schor, J.L. Reid, C.E. MacPhee, N.R. Stanley-Wall, The diverse structures and functions of surfactant proteins, Trends Biochem. Sci. 41 (2016) 610–620, https:// doi.org/10.1016/j.tibs.2016.04.009.

[37] J.M. Ruso, J. Piñeiro, Proteins in Solution and at Interfaces, John Wiley & Sons, Inc., Hoboken, NJ, USA, 2013, https://doi.org/10.1002/9781118523063.

[38] C.D. Mackenzie, B.O. Smith, A. Meister, A. Blume, X. Zhao, J.R. Lu, M.W. Kennedy, A. Cooper, Ranaspumin-2: structure and function of a surfactant protein from the foam nests of a tropical frog, Biophys. J. 96 (2009) 4984–4992, https://doi.org/10. 1016/j.bpj.2009.03.044.

[39] C.D. Mackenzie, B.O. Smith, A. Meister, A. Blume, X. Zhao, J.R. Lu, M.W. Kennedy, A. Cooper, Ranaspumin-2: structure and function of a surfactant protein from the foam nests of a tropical frog, Biophys. J. 96 (2009) 4984–4992, https://doi.org/10.1016/j.bpj.2009.03.044.

[40] D. Kredi, Improving Interfaces for Nerve Repair, (2016).

[41] B.O. Desai, V. Kredi, D. Riehle, M.O. Smith, Application of natural surfactant protein fusions to direct cell adhesion on hydrophobic substrates, Eur. Biophys. J. 46 (2017) 328, https://doi.org/10.1007/s00249-017-1222-x.

Published in : Colloids and Surfaces B: Biointerfaces (2019), vol. 178, pp. 120–128
DOI: 10.1016/j.colsurfb.2019.02.049
Status : Postprint (Author's version)

[42] G.F. Trindade, M. Abel, J.F. Watts, simsMVA: a tool for multivariate analysis of ToF-SIMS datasets, Chemometr. Intell. Lab. Syst. (2018), https://doi.org/10.1016/j. chemolab.2018.10.001.

[43] S. Zhu, Y. Tian, A.E. Hamielec, D.R. Eaton, Radical concentrations in free radical copolymerization of MMA/EGDMA, Polymer (Guildf.) 31 (1990) 154–159, https://doi.org/10.1016/0032-3861(90)90368-9.

[44] T.G. Carswell, D.J.T. Hill, R. Kellman, D.I. Londero, J.H. O'Donnell, P.J. Pomery, C.L. Winzor, Mechanisms of polymerization of methacrylate copolymers of biological interest, Makromol. Chem. Macromol. Symp. 51 (1991) 183–191, https://doi. org/10.1002/masy.19910510116.

[45] E. Vivaldo-Lima, Modeling of the free-radical copolymerization kinetics with crosslinking of methyl methacrylate / ethylene glycol dimethacrylate up to high conversions and considering thermal effects, Rev. Soc. Quím. Méx. 47 (2003) 22–33.

[46] P. Cools, S. Van Vrekhem, N. De Geyter, R. Morent, The use of DBD plasma treatment and polymerization for the enhancement of biomedical UHMWPE, Thin Solid Films 572 (2014) 251–259, https://doi.org/10.1016/j.tsf.2014.08.033.

[47] R. Luo, L. Tang, J. Wang, Y. Zhao, Q. Tu, Y. Weng, R. Shen, N. Huang, Improved immobilization of biomolecules to quinone-rich polydopamine for efficient surface functionalization, Colloids Surf. B Biointerfaces 106 (2013) 66–73, https://doi.org/ 10.1016/j.colsurfb.2013.01.033.

[48] E.A. Pillar, R. Zhou, M.I. Guzman, Heterogeneous oxidation of catechol, J. Phys. Chem. A 119 (2015) 10349–10359, https://doi.org/10.1021/acs.jpca.5b07914.

[49] T. Vo-dinh, Biomedical Photonics, (2003), p. 1787, https://doi.org/10.1117/1. 1776177.

[50] Q. Ye, F. Zhou, W. Liu, Bioinspired catecholic chemistry for surface modification, Chem. Soc. Rev. 40 (2011) 4244–4258, https://doi.org/10.1039/c1cs15026j.

[51] E. Faure, C. Falentin-Daudré, C. Jérôme, J. Lyskawa, D. Fournier, P. Woisel, C. Detrembleur, Catechols as versatile platforms in polymer chemistry, Prog. Polym. Sci. 38 (2013) 236–270, https://doi.org/10.1016/j.progpolymsci.2012.06.004.

[52] Y. Li, S. Jongberg, M.L. Andersen, M.J. Davies, M.N. Lund, Quinone-induced protein modifications: kinetic preference for reaction of 1,2-benzoquinones with thiol groups in proteins, Free Radic. Biol. Med. 97 (2016) 148–157, https://doi.org/10.1016/j.freeradbiomed.2016.05.019.

[53] J. Yang, M.A. Cohen Stuart, M. Kamperman, Jack of all trades: versatile catechol crosslinking mechanisms, Chem. Soc. Rev. 43 (2014) 8271–8298, https://doi.org/ 10.1039/C4CS00185K.

[54] R.J. Morris, G.B. Brandani, V. Desai, B.O. Smith, M. Schor, C.E. MacPhee, The conformation of interfacially adsorbed Ranaspumin-2 is an arrested state on the unfolding pathway, Biophys. J. 111 (2016) 732–742, https://doi.org/10.1016/j.bpj.2016.06.006.